

Weakly-Supervised Domain Adaptation of Deep Regression Trackers via Reinforced Knowledge Distillation

Matteo Dunnhofer, Niki Martinel, and Christian Micheloni

Abstract—Deep regression trackers are among the fastest tracking algorithms available, and therefore suitable for real-time robotic applications. However, their accuracy is inadequate in many domains due to distribution shift and overfitting. In this paper we overcome such limitations by presenting the first methodology for domain adaptation of such a class of trackers. To reduce the labeling effort we propose a weakly-supervised adaptation strategy, in which reinforcement learning is used to express weak supervision as a scalar application-dependent and temporally-delayed feedback. At the same time, knowledge distillation is employed to guarantee learning stability and to compress and transfer knowledge from more powerful but slower trackers. Extensive experiments on five different robotic vision domains demonstrate the relevance of our methodology. Real-time speed is achieved on embedded devices and on machines without GPUs, while accuracy reaches significant results.

Index Terms—Visual Tracking; Computer Vision for Automation; Deep Learning for Visual Perception

I. INTRODUCTION

REAL-TIME visual object tracking is a key module in many robotic perception systems [1], [2], [3], [4], [5], [6]. Recently, deep regression trackers [7], [8], [9] (DRTs) have been proposed in the robotics community [7] because of their efficiency and generality. Thanks to their simple architecture, DRTs achieve processing speeds that surpass 100 FPS, making them suitable even for low-resource robots. Moreover, with the availability of large-scale computer vision datasets [10], these trackers can learn to track a large variety of targets without relying on particular assumptions, thus simplifying the development of tracking pipelines. However, acquiring thousands of videos for training these systems is not realistic in many real-world robotic application domains. Additionally, many domains offer particular scenarios that differ much from the examples which DRTs are trained on. For example, drone [11] and driving [3], [12] applications require tracking objects from particular camera views. Underwater robots offer uncommon targets and settings [4], [13]. Other robotics systems can use different imaging modalities [2]. Robotic manipulation

Manuscript received: December, 4th, 2020; Revised February, 25th, 2021; Accepted March, 25th, 2021.

This paper was recommended for publication by Editor Eric Marchand upon evaluation of the Associate Editor and Reviewers' comments. This work was supported by the ACHIEVE-ITN H2020 project.

All authors are with Machine Learning and Perception Lab, University of Udine, Udine, Italy. Matteo Dunnhofer's e-mail matteo.dunnhofer@uniud.it

Digital Object Identifier (DOI): see top of this page.

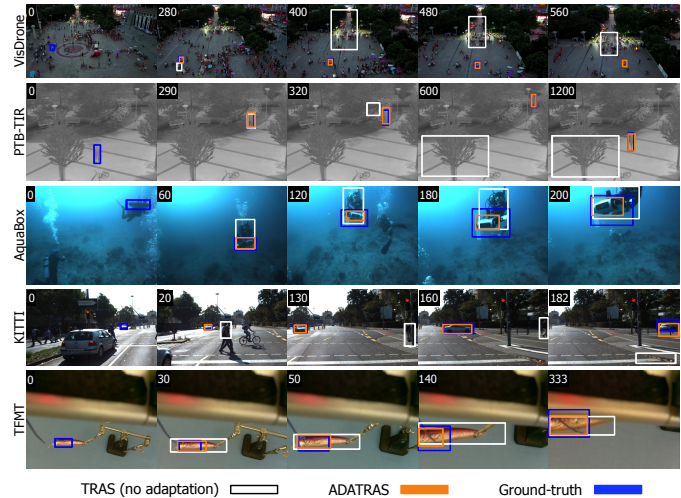


Fig. 1: We propose a weakly-supervised strategy to adapt DRTs for particular and small-data robotic applications. This figure shows the performance of the TRAS tracker against its adapted version ADATRAS on five different robotic tracking settings. For better visualization, please check out the video at this link <https://youtu.be/3T3BJudDSwQ>.

configurations need the tracking of atypical objects [14]. As shown in Figure 1, these situations cause DRTs' accuracy to be very low. This is due to their deep learning architecture that is subject to overfitting if trained directly on small application datasets, and suffers from the shift between training and test data distributions when trained for large-scale generic object tracking.

To address these issues, the visual tracking community proposes to increase the learning capacity of convolutional neural networks [15] (CNNs), or to use online learning mechanisms to adapt the capabilities of deep trackers [16], [17], [18] to every new target in every new video. These strategies lead to higher accuracy and robustness, but at cost of real-time speed achieved just on high-end machines. On the other hand, transfer learning [19] and domain adaptation [20] are widely used machine learning techniques to address such issues. The idea is to exploit the knowledge acquired in a source domain and adapt it to new target domains through an additional offline learning stage that exploits a few examples of the target domain. This allows to improve performance and generalization on the new domains, without sacrificing the test-time processing speed, as the deep models can be applied without any additional tuning. Different solutions have

been proposed to adapt robotic vision systems [21], [22], [23], but no work considered adaptation in the context of robotic tracking.

Considering these motivations, the main contribution of this paper is the first methodology for offline domain adaption of DRTs. This is also the first work that considers the domain adaptation problem in the context of visual tracking. To reduce the labeling effort and maintain application-specific development, we propose a weakly-supervised adaptation procedure. Thanks to reinforcement learning (RL), the knowledge previously acquired in a generic object tracking domain is adjusted with scalar signals that can be also delayed in time. But, as RL optimization is difficult, we build upon the experience of more accurate but slower trackers via knowledge distillation (KD) to stabilize learning and additionally improve the performance. We build our solution on the recent framework proposed in [9], which marries KD and RL for generic object tracking. However, such a method is designed for learning DRTs with bounding-box level and densely annotated datasets. Hence, as an additional contribution, in this paper we offer a generalization of [9] that allows its exploitation in weakly labeled settings and for generic application objectives. Extensive analysis on five different robotic tracking domains shows that the proposed adaptation strategy makes DRTs applicable again on particular and low-resource robotic perception domains.

II. RELATED WORK

Domain Adaptation in Robotic Vision. Domain adaptation has been previously studied in robotic vision. Spatial information about the domains has been exploited to adapt robotic vision system to recognize new objects [21]. Wulfmeier et al. [24] used adversarial approaches to adapt segmentation models to the visual appearance of weather and seasonal conditions. Batch normalization layers have been exploited for robotic vision-based kitting [25]. Particular loss functions [26], [22], augmentation networks [23], or pretext tasks [27] have been proposed extensively for the adaptation of visual capabilities from simulated to real environments. Bellocchio et al. [28] used generative adversarial networks to adapt robotic fruit counting systems to unseen species. Yet, no work considered the problem of adapting tracking knowledge acquired in a generic domain to another different robotic target domain. Furthermore, no method mixing RL and KD has been introduced in the context of domain adaptation.

Adaptation in Visual Tracking. In the visual tracking panorama, the concept of domain adaptation has been used to refer to instance-level online learning performed on the target object of every new test sequence. MDNet-based trackers [16] consider a training sequence as a domain and propose a CNN learned offline via binary classification on multiple domain-specific branches. Such a model is then refined on every test sequence by solving an online binary classification problem. ATOM [17] combines an offline learned bounding-box regression model with an efficient target-background IoU-based discriminator which is trained exclusively online. DiMP [18] performs an online update of a target-specific CNN model via a fast discriminative-learning optimization strategy. With

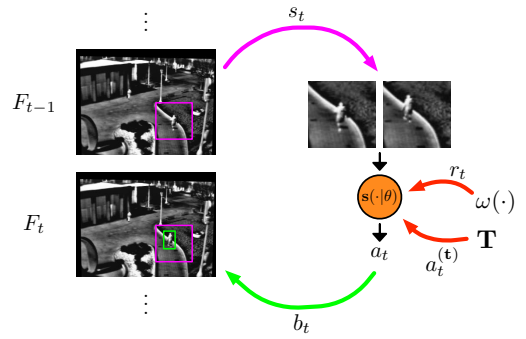


Fig. 2: Visual representation of the MDP interaction process between the student and a video. At each step t , a state s_t is extracted from frames F_{t-1}, F_t . s_t is processed by s which outputs the action a_t that is transformed into the bounding-box output b_t . During the adaptation procedure, the learning is driven by the weak supervision function $\omega(\cdot)$ and by the actions of the set of teacher trackers \mathbf{T} .

respect to these works, our solution is conceptually different. We consider the target domain as a set of videos whose a subset is dedicated to offline learning. This introduces an additional training procedure, but it allows the adapted tracker to be extremely fast at test time, thanks to the avoidance of online adaptation mechanisms that reduce the tracking speed.

III. METHODOLOGY

We build our solution upon the recent framework of [9], which showed the effectiveness of combining KD and RL for generic object tracking. Differently from [9], in this paper, we use RL to express a weak and temporally-delayed application-specific objective and employ KD to make the convergence achievable. We remark that our methodology of [9] is not applicable as it is for our problem, because it assumes a fully supervised setting in which dense ground-truth bounding-box data is available.

Preliminaries and Problem Statement. We consider a video $\mathcal{V}_j = \{F_t \in \mathcal{I}\}_{t=0}^{T_j}$ as a sequence of frames, where each F_t belongs to the space of RGB images $\mathcal{I} = \{0, \dots, 255\}^{w \times h \times 3}$. Each video has a target object to be tracked, which is defined in the first frame F_0 through a bounding-box $b_0^{(g)} = [x_0^{(g)}, y_0^{(g)}, w_0^{(g)}, h_0^{(g)}] \in \mathbb{R}^4$ that specifies the coordinates of the object's top left corner, and its width and height. The goal of a tracker, given each frame F_t , is to predict the bounding-box $b_t = [x_t, y_t, w_t, h_t]$ that best fits the target in F_t .

As our solution is based on the KD framework, we employ the concepts of student and teacher [29]. We formally consider a regression-based tracker as the student $s : \mathcal{I} \times \mathcal{I} \times \Theta \rightarrow \mathbb{R}^4$ which is a function parameterized by $\theta \in \Theta$ that outputs the relative motion of the target contained in two consecutive images given as input. We assume the student has acquired general tracking knowledge by optimizing θ on the videos of a source domain $\mathcal{D}^{(\text{source})}$. The set of teachers is defined as $\mathbf{T} = \{\mathbf{t} : \mathcal{I} \rightarrow \mathbb{R}^4\}$ where each \mathbf{t} is a generic tracking function that, given a frame, produces a bounding-box for that frame.

Our problem of interest consists in adapting $s(\cdot|\theta)$'s past ability to a new tracking domain $\mathcal{D}^{(\text{target})}$ different from

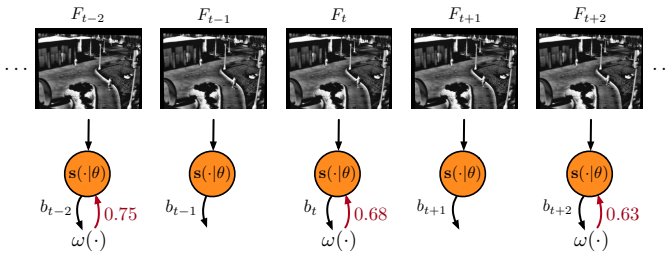


Fig. 3: Visual representation of the student’s feedback mechanism based on the weak supervision function $\omega(\cdot)$. At every t , $s(\cdot|\theta)$ gives its bounding-box prediction b_t which is eventually evaluated with a 0-1 score by $\omega(\cdot)$ (if $\omega(\cdot)$ is defined for that temporal step).

$\mathcal{D}^{(\text{source})}$. More specifically, we assume $\mathcal{D}^{(\text{target})}$ is split into a training set $\mathcal{D}_{tr}^{(\text{target})} \subseteq \mathcal{D}^{(\text{target})}$, and a test set $\mathcal{D}_{te}^{(\text{target})} \subseteq \mathcal{D}^{(\text{target})}$ with $\mathcal{D}_{tr}^{(\text{target})} \cap \mathcal{D}_{te}^{(\text{target})} = \emptyset$. The goal is to exploit $\mathcal{D}_{tr}^{(\text{target})}$, for which weak supervision is given, to maximize the tracking performance on the videos of $\mathcal{D}_{te}^{(\text{target})}$.

Video Processing. To use RL, we model the tracking as an interaction process [30]. We treat $s(\cdot|\theta)$ as an artificial agent which interacts with a video $\mathcal{V}_j \in \mathcal{D}^{(\text{target})}$ according to the Markov Decision Process (MDP) definition given in [9]. The interaction happens as a temporal sequence of states s_1, s_2, \dots, s_t , and actions a_1, a_2, \dots, a_t . Every s_t is defined as a pair of image patches obtained by cropping F_{t-1} and F_t using the previously known bounding-box b_{t-1} and a factor c that enlarges the patches in order to include additional image context information. At the t -th step, the student is given the state s_t and outputs the continuous action a_t . Each a_t is defined as the vector $a_t = [\Delta x_t, \Delta y_t, \Delta w_t, \Delta h_t] \in [-1, 1]^4$ which quantifies the relative horizontal and vertical translations ($\Delta x_t, \Delta y_t$, respectively) and width and height scale variations ($\Delta w_t, \Delta h_t$, respectively) that have to be applied to b_{t-1} to predict b_t . Hence, based on the previous bounding-box estimate [9], a_t is transformed into the bounding-box b_t which provides the localization of the target in frame F_t . A visual representation of the interaction procedure is depicted in Figure 2.

Weak Supervision. During adaptation on videos $\mathcal{V}_j \in \mathcal{D}_{tr}^{(\text{target})}$, the actions a_t of s are rewarded by the scalar value $r_t \in [-1, 1]$ (in RL terms, the reward). In our setting, this is what we use to express weak supervision. Differently from [9], who proposed a continuously available bounding-box overlap formulation, we just assume the feedback to be released as a 0-1 value through an arbitrary function $\omega : \mathbb{R}^4 \rightarrow [0, 1]$ that evaluates a bounding-box prediction b_t and that can be implemented based on the application needs. Additionally, we do not require $\omega(b_t)$ to be defined for every t . $\omega(b_t)$ is formally exploited in our proposed MDP reward definition which, at every t , is

$$r_t = r(b_t) = \begin{cases} 0 & \text{if } \omega(b_t) \text{ is not defined} \\ \nu(\omega(b_t)) & \text{if } \omega(b_t) \text{ is defined } \wedge \omega(b_t) \geq 0.5 \\ -1 & \text{otherwise} \end{cases} \quad (1)$$

with $\nu(z) = 2(\lfloor z \rfloor_{0.05}) - 1$ that floors to the closest 0.05 digit and shifts the input range from $[0, 1]$ to $[-1, 1]$. Figure 3 visualizes the proposed weak supervision mechanism.

Adapting the Tracker. The student’s parameters θ , which have been pretrained on the $\mathcal{D}^{(\text{source})}$, are adapted to $\mathcal{D}^{(\text{target})}$ by learning offline on $\mathcal{D}_{tr}^{(\text{target})}$. To do this, we employ the end-to-end strategy proposed in [9] and we briefly report it by highlighting the improvements that allow its generalization for weak supervision.

Our adaptation strategy provides two learning objectives that are fulfilled at the same time. To optimize the actions with respect to $\omega(\cdot)$ (by means of the rewards), the following RL actor-critic loss formulation [31]

$$\mathcal{L}_{\text{RL}} = \mathcal{L}_{\pi} + \mathcal{L}_v \quad (2)$$

$$\mathcal{L}_{\pi} = - \sum_{i=1}^{t_{max}} \log s(s_i|\theta) (r_i + \gamma s_v(s_{i+1}|\theta) - s_v(s_i|\theta)) \quad (3)$$

$$\mathcal{L}_v = \sum_{i=1}^{t_{max}} \frac{1}{2} (R_i - s_v(s_i|\theta))^2, R_i = \sum_{k=1}^i \gamma^{k-1} r_k \quad (4)$$

is applied after t_{max} steps of interaction with $\mathcal{V}_j \in \mathcal{D}_{tr}^{(\text{target})}$, in which each a_t performed by s is sampled from a normal distribution $\mathcal{N}(\mu, \sigma)$. To attend this optimization goal, the student is set to produce the additional output $v_t = s_v(s_t|\theta)$, which is the prediction of the γ -discounted cumulative reward R_i that s expects to receive from s_t to the end of the interaction. In RL terms, \mathcal{L}_{π} and \mathcal{L}_v are known as policy gradient loss with advantage and value loss respectively.

On a second side, our adaptation scheme minimizes the following objective

$$\mathcal{L}_{\text{KD}} = \sum_{i=1}^{t_{max}} |a_i^{(t)} - s(s_i|\theta)| \cdot m_i, \quad (5)$$

which is the L1 loss [7], [8] between the actions performed by s and the actions $a_i^{(t)}$ that the teacher would take to move s ’s bounding-box b_{t-1} into the t ’s prediction $b_t^{(t)}$ [9]. Each of the differences in Eq. (5) are multiplied by the binary values m_i which represent the case in which s performs worse than the teacher. This learning objective makes the learning feasible and has the additional advantage of extracting knowledge from more accurate and robust tracking algorithms, leading ultimately to better performance. A distributed setting [32] is employed to implement the overall optimization strategy by considering $\frac{\xi}{2}$ students for the optimization of Eq. (2) and the other $\frac{\xi}{2}$ for Eq. (5).

The proposed adaptation procedure brings some modifications to the learning method of [9] that it allows to work in weakly supervised settings. First, the policy gradient $\log s(s_i|\theta)$ term used in Eq. (3) is obtained after the definition of a normal distribution $\mathcal{N}(\mu, \sigma)$ with mean defined as $\mu = s(s_t|\theta)$ and standard deviation σ considered with a fixed value. In this way, varying σ one can control s ’s exploration without the need of ground-truth bounding-boxes as in [9]. Second, we propose to favor t ’s prediction in the computation of $m_i \in \{0, 1\}$ of Eq. (5), by setting $m_i = 1$ if $r(b_t^{(t)}) \geq r(b_t)$ holds and $m_i = 0$ otherwise. This in order to address the 0

TABLE I: Statistics of the target domains selected for this work. The number of training and test videos, frames, and the number of sequences after splitting the videos in chunks of 32 frames, are reported in the first five rows. SS and PS obtained by the teachers on the training videos are reported in the last three rows.

Target Domain	VisDrone	PTB-TIR	AquaBox	KITTI	TFMT
$ \mathcal{D}_{tr}^{(target)} $	86	48	41	21	6
$ \mathcal{D}_{te}^{(target)} $	11	12	20	20	6
# frames $\mathcal{D}_{tr}^{(target)}$	69941	23497	3927	4797	520
# frames $\mathcal{D}_{te}^{(target)}$	7046	6532	6033	4143	1320
# splitted sequences $\mathcal{D}_{tr}^{(target)}$	1696	804	263	356	42
$\mathbf{T}_V \mathcal{D}_{tr}^{(target)}$ SS PS	0.556 0.798	0.565 0.817	0.321 0.488	0.385 0.668	0.283 0.385
$\mathbf{T}_S \mathcal{D}_{tr}^{(target)}$ SS PS	0.576 0.741	0.617 0.785	0.499 0.717	0.430 0.579	0.460 0.659
$\mathbf{T}_A \mathcal{D}_{tr}^{(target)}$ SS PS	0.555 0.759	0.559 0.691	0.563 0.843	0.450 0.619	0.619 0.783

reward scenarios caused by the non definition of $\omega(\cdot)$, in which it is not possible to infer the actual student performance. Third, the \mathbf{t} to which learn from in Eq. (5) is selected before the start of the interaction via some arbitrary decision strategy that can be defined depending on the application objectives and resources.

Tracking after Adaptation. After the adaptation-by-learning process is done, the student $\mathbf{s}(\cdot|\theta)$ is ready to be used for tracking on $\mathcal{D}_{te}^{(target)}$ as follows. We consider each testing video $\mathcal{V}_j \in \mathcal{D}_{te}^{(target)}$, for which the target is individuated in F_0 by the bounding-box $b_0^{(g)}$, as the aforementioned MDP. At each t , s_t are extracted from F_{t-1}, F_t , and a_t are performed by means of the student’s adapted policy $\mathbf{s}(s_t|\theta)$ and transformed into bounding-box outputs b_t . We name the tracker resulting from this tracking procedure ADATRAS (ADAPted TRACKing Student).

IV. EXPERIMENTAL SETUP

Performance Measures. To evaluate the performance of the trackers involved in this paper, we follow the standard methodology introduced in [33]. Trackers are initialized in the first frame of a sequence with the target ground-truth bounding-box and let run until the end, respecting the one-pass evaluation (OPE) protocol. The quantitative measures used are the area under the curve (AUC) of the success and precision plots, which are referred as to success score (SS) and precision score (PS) respectively.

Tracker. We follow the most recent advancements in deep regression tracking [7], [34], [9] to implement our tracker $\mathbf{s}(\cdot|\theta)$ as a deep neural network with weights θ . The network gets as input s_t as two image patches which pass through two ResNet-18 [35] CNN branches with shared weights. The subsequent feature maps are linearized, concatenated together, and fed to two consecutive fully connected layers with ReLU activations and an LSTM layer [36], both with 512 neurons. The LSTM’s output is finally fed to two fully connected heads that output the action $a_t = \mathbf{s}(s_t|\theta)$ and the state-value $v_t = \mathbf{s}_v(s_t|\theta)$ respectively.

Source and Target Domains. We conducted experiments considering the GOT-10k [37] and LaSOT [38] benchmarks as source domains $\mathcal{D}^{(source)}$. These are large-scale tracking datasets containing, respectively, 10000 and 1400 videos of generic target objects (up to 563 to different object classes)

in generic tracking settings. The initial optimization of θ on these sets was performed following the details of [9].

We demonstrate the capabilities of our solution on five robotic target domains, which we refer to as VisDrone, PTB-TIR, AquaBox, KITTI, and TFMT. These were selected due to their particular characteristics in: camera views; uncommon objects and motions; image modality. Statistics of the domains are shown in Table I. Beside being real-world robotic vision datasets, these domains also contain bounding-box labels for every frame of the videos. This permits an accurate validation with the control and simulation of the loss of supervision.

a) *VisDrone*: This domain concerns tracking objects in videos acquired from drones, and it is based on the publicly available VisDrone 2019 challenge dataset [39]. Targets available are persons, cars, or animals, acquired by particular camera views in which they appear very small and their motion is different depending on the drone’s altitude. To implement $\mathcal{D}_{tr}^{(target)}$ and $\mathcal{D}_{te}^{(target)}$ we employed, respectively, the original training and validation sets provided by the authors [39].

b) *PTB-TIR*: The PTB-TIR target domain regards tracking people in videos acquired through a thermal-infrared (TIR) camera. This domain offers common objects (people), but video frames are represented via a different sensor. The data contained in the PTB-TIR benchmark [40] was employed. $\mathcal{D}_{tr}^{(target)}$ and $\mathcal{D}_{te}^{(target)}$ were obtained by randomly splitting, with an 80-20 ratio, the 60 videos contained in the benchmark.

c) *AquaBox*: This domain consists in tracking an underwater robot in an underwater video setting. Videos offer targets, camera views, motions, and object physics, that are very unusual from what available in standard tracking datasets. The data used was obtained with the AquaBox dataset [4]. For $\mathcal{D}_{tr}^{(target)}$ and $\mathcal{D}_{te}^{(target)}$ we employed the training and validation sets provided by the authors. Only videos composed of at least 25 frames were retained.

d) *KITTI*: This domain concerns tracking vehicles and people in videos acquired from a vehicle point of view, thus offering new camera views (different from the drone’s) on common objects. We used the popular KITTI dataset [3] to implement $\mathcal{D}_{tr}^{(target)}$ and $\mathcal{D}_{te}^{(target)}$. We considered tracks longer than 100 frames of the KITTI’s training videos and splitted them with a 50% ratio.

e) *TFMT*: This target domain requires tracking objects to perform a fine grained manipulation task with a robotic arm [14]. The targets and the settings contained in this dataset are very uncommon to generic object trackers. The 12 labeled

TABLE II: Comparison between ADATRAS and the teachers and DRTs. FPS are obtained on the SM machine. Best results, per domain and performance measure, are highlighted in red, second-best in blue, third-best in green.

Tracker	VisDrone			PTB-TIR			AquaBox			KITTI			TFMT		
	SS	PS	FPS	SS	PS	FPS	SS	PS	FPS	SS	PS	FPS	SS	PS	FPS
MDNet [16]	0.559	0.902	2	0.586	0.953	2	0.543	0.504	2	0.413	0.686	3	0.501	0.770	2
SiamRPN++ [15]	0.532	0.790	31	0.614	0.774	55	0.591	0.753	41	0.504	0.632	43	0.504	0.637	27
ATOM [17]	0.539	0.891	16	0.620	0.778	24	0.594	0.742	20	0.529	0.686	19	0.615	0.639	28
GOTURN [8]	0.350	0.600	56	0.327	0.497	200	0.402	0.468	110	0.209	0.313	62	0.363	0.271	125
RE3 [7]	0.354	0.626	60	0.201	0.278	255	0.445	0.398	107	0.221	0.308	63	0.406	0.272	136
TRAS [9]	0.384	0.653	65	0.432	0.603	168	0.522	0.619	161	0.486	0.627	85	0.332	0.169	112
ADATRAS	0.552	0.823	67	0.661	0.862	170	0.576	0.732	165	0.537	0.720	89	0.581	0.659	115

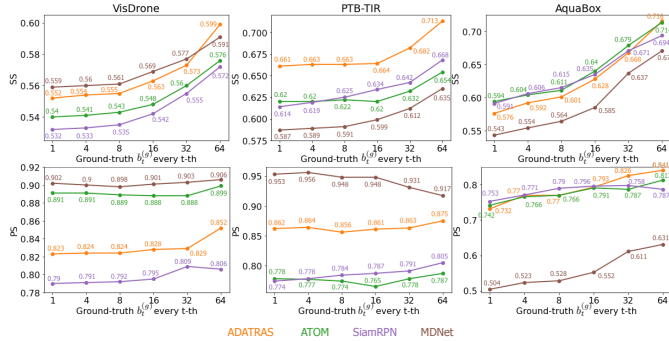


Fig. 4: Effect of evaluating the trackers with a weakly-labeled test set in which ground-truths are available every 4-th, 8-th, 16-th, 32-th, and 64-th frame.

videos contained in the TFMT dataset [14] have been splitted with a 50% ratio to implement $\mathcal{D}_{tr}^{(target)}$ and $\mathcal{D}_{te}^{(target)}$.

Weak Supervision Form. We experimented two forms of 0-1 function to weakly supervise $s(\cdot|\theta)$. The first implements ω as the function $\omega^{(iou)}(b_t, b_t^{(g)}) = \text{IoU}(b_t, b_t^{(g)})$, which takes the student’s predicted bounding-box and a bounding-box reference $b_t^{(g)}$ of the target and computes their intersection-over-union as

$$\text{IoU}(b_t, b_t^{(g)}) = (b_t \cap b_t^{(g)}) / (b_t \cup b_t^{(g)}). \quad (6)$$

The second form is through the 0-1 function $\omega^{(dist)}(b_t, b_t^{(g)}) = 1 - \text{NormDist}(b_t, b_t^{(g)})$ where

$$\text{NormDist}(b_t, b_t^{(g)}) = \frac{\sqrt{(x_t - x_t^{(g)})^2 + (y_t - y_t^{(g)})^2}}{20} \quad (7)$$

is the function that computes the pixel distance between the centers of b_t and $b_t^{(g)}$, truncated at 20 and normalized by the same value. The value 20 was chosen following the standard precision score threshold defined in [33].

Teachers. The tracking teachers selected for this work are MDNet [16], SiamRPN++ [15], and ATOM [17]. Since they tackle visual tracking by different approaches, it is more likely that at least one can succeed in the application domain, and thus provide useful tracking knowledge. In the experiments, we considered exploiting single teachers or a pool of teachers. In particular, the following sets of teachers were examined $\mathbf{T}_M = \{\text{MDNet}\}$, $\mathbf{T}_S = \{\text{SiamRPN++}\}$, $\mathbf{T}_A = \{\text{ATOM}\}$, $\mathbf{T}_P = \{\text{MDNet}, \text{SiamRPN++}, \text{ATOM}\}$. The performance of these on $\mathcal{D}_{tr}^{(target)}$ are shown in the last three rows

of Table I. We studied two methods to select the teacher \mathbf{t} in Eq. (5). The first randomly selects $\mathbf{t} \in \mathbf{T}$ using a uniform distribution. The second selects \mathbf{t} based on the average $\omega(\cdot)$ performance, that is

$$\mathbf{t} \in \mathbf{T} : \Omega(\mathbf{t}, \mathcal{V}_j) = \max_{\mathbf{t} \in \mathbf{T}} \Omega(\mathbf{t}, \mathcal{V}_j) \quad (8)$$

where

$$\Omega(\mathbf{t}, \mathcal{V}_j) = \frac{\sum_{t=0}^{T_j} \omega(b_t^{(\mathbf{t})})}{T_j} \quad (9)$$

is a 0-1 number that estimates the quality of \mathbf{t} ’s predictions given for video $\mathcal{V}_j \in \mathcal{D}_{tr}^{(target)}$.

Implementation Details. To produce more training samples, each video (and the respective filtered bounding-box sequences) was split in 20 randomly indexed sequences of 32 frames, following [7], [9]. The total number of videos is reported in row five of Table I. A temporal reverse of the sequences was also applied with 50% probability during training. $S = 12$ training students were used for training. $\sigma = 0.05$ was set for the VisDrone PTB-TIR, KITTI, and TFMT domains, and $\sigma = 0.025$ for AquaBox. To facilitate the learning, a curriculum learning procedure similar to [7] was employed by increasing the length of the interaction during the adaptation procedure. The Adam optimizer [41] was utilized. A learning rate of $7.5 \cdot 10^{-7}$ was set for all the layers of the student except for the fully connected layer that predicts v_t , for which learning rate was set to 10^{-5} . The student was trained until the validation performance stopped improving. Trainings took between 12 and 48 hours, depending on the amount of data available in a domain. We experienced some variance between the outcomes of different experiment runs, and therefore we report averaged results. Other settings not specified in this section have been inherited from [9]. In the following of the paper, if not specified otherwise, default experimental settings are with the student initially optimized on GOT-10k-based $\mathcal{D}^{(source)}$, learning from \mathbf{T}_P by respecting Eq. (8), with weak supervision based on $\omega^{(iou)}(\cdot)$ given at every time step, and with the hyper-parameters mentioned above.

Hardware and Software. We employed three hardware machines for our experiments. A high-end server machine with an Intel Xeon E5-2690 v4 @ 2.60GHz CPU, 320 GB of RAM, and 4 NVIDIA TITAN V GPUs. We refer to this as SM. A desktop computer with an Intel Xeon W-2125 @ 4.00GHz CPU, 32GB of RAM, and an NVIDIA GTX1080-Ti, which we refer to as DM. And an embedded board NVIDIA Jetson

TABLE III: Speed performance in FPS of ADATRAS and the teachers on different machines. Best results, per machine, are highlighted in bold. (ATOM w/o GPU results were not obtained because the implementation was not designed to run without it.)

Tracker		VisDrone			PTB-TIR			AquaBox		
		SM	DM	ED	SM	DM	ED	SM	DM	ED
MDNet [16]	w GPU	2	3	< 1	2	3	< 1	2	3	< 1
	w/o GPU	< 1	< 1	< 1	< 1	< 1	< 1	< 1	< 1	< 1
SiamRPN++ [15]	w GPU	31	28	1	55	43	1	41	35	1
	w/o GPU	3	3	< 1	3	3	< 1	3	3	< 1
ATOM [17]	w GPU	16	28	3	24	59	4	20	43	4
	w/o GPU	-	-	-	-	-	-	-	-	-
ADATRAS	w GPU	67	80	15	170	216	23	165	185	26
	w/o GPU	33	55	2	62	91	2	98	168	2

TABLE IV: Comparison of the proposed weakly-supervised domain adaptation method (last row) with baselines that: do not adapt; are trained from scratch; do fine-tuning. Best results, per method, are highlighted in bold.

Method	VisDrone		PTB-TIR		AquaBox	
	SS	PS	SS	PS	SS	PS
no adaptation (TRAS)	0.384	0.653	0.432	0.603	0.522	0.619
from scratch by [9]	0.459	0.712	0.585	0.751	0.601	0.670
fine-tuning by [9]	0.549	0.795	0.659	0.848	0.569	0.762
from scratch by proposed	0.475	0.722	0.625	0.819	0.549	0.695
adaptation by proposed	0.552	0.823	0.661	0.862	0.576	0.732

Nano with an ARM A57 quad-core 1.43 GHz CPU, 4GB of RAM, and a Maxwell 128 core GPU, which we refer to as ED. All the code was implemented in Python. Trainings were performed on the SM machine.

V. RESULTS

Comparison with other Trackers. Table II reports the performance of ADATRAS in comparison with teachers and other DRTs on the considered robotic domains. After adaptation, our proposed tracker competes with the top-performing trackers generally. On some domains (e.g. PTB-TIR, KITTI) it also outperforms them. Regarding the processing speed, ADATRAS is always faster than these methods. The performance of TRAS [9], RE3 [7] and GOTURN [8] demonstrate the difficulties of DRTs due to the domain shift. In Figure 1, qualitative results of ADATRAS in comparison with the non adapted TRAS are presented. Given these results, our methodology allows to make DRTs accurate as state-of-the-art visual trackers in challenging robotic vision domains.

We analyse in depth our methodology on the VisDrone, PTB-TIR, AquaBox domains from now on. Figure 4 shows how the performance of ADATRAS and the teachers change considering weak supervision also for $\mathcal{D}_{te}^{(target)}$. In particular, the SS and PS performance was analyzed with ground-truths $b_t^{(g)}$ available every 4-th, 8-th, 16-th, 32-th, and 64-th frame. Overall, the performance tends to increase as fewer references are used for evaluation, especially for domains with a smaller number of frames. For some less-frequent $b_t^{(g)}$ settings, ADATRAS results more accurate than the teachers.

Speed Analysis. Table III reports the analysis on the processing speed of our method in comparison with the teachers on different machines. ADATRAS results the fastest method on all machine setups. Very high speeds are reached on top machines with a GPU (SM or DM), leaving large space for

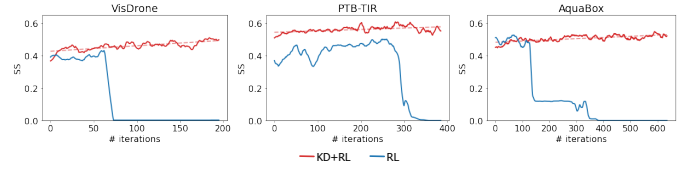


Fig. 5: SS trends on $\mathcal{D}_{te}^{(target)}$ of the proposed adaptation strategy (red line) and a pure RL fine-tuning (blue line) at different iterations during the learning phase. After some iterations, the RL-based solution diverges, while the proposed adaptation continuously improves ADATRAS (as shown by the red dashed line). Lines have been smoothed for better visualization.

TABLE V: Performance comparison between ADATRAS and trackers fine-tuned on $\mathcal{D}_{tr}^{(target)}$. Best results, per tracker, are highlighted in bold.

Tracker	VisDrone		PTB-TIR		AquaBox	
	SS	PS	SS	PS	SS	PS
SiamRPN++-ft [15]	0.594	0.842	0.572	0.733	0.559	0.703
GOTURN-ft [8]	0.380	0.642	0.353	0.548	0.450	0.374
RE3-ft [7]	0.168	0.297	0.408	0.554	0.530	0.586
ADATRAS	0.552	0.823	0.661	0.862	0.576	0.732

real-time downstream application development and making it good for lower resource robots. Remarkably, ADATRAS achieves real-time speed even without a GPU when run on top machines. When run on small embedded devices like ED, ADATRAS achieves real-time speeds on PTB-TIR and AquaBox and a quasi-real-time speed on VisDrone, considering 20 FPS as real-time baseline [42], [43].

Comparison with Baselines. Table IV presents the performance of our methodology in comparison with baseline adaptation and no-adaptation methods. Our method (in the last row) outperforms the tracker without adaptation (TRAS [9]) on every target domain. These results show that the goal of improving the baseline tracker’s accuracy with weak supervision is achieved. Generally, performance is even improved with respect to the dense bounding-box supervision experiments performed following [9], thus justifying the introduced improvements. Adapting past knowledge is effective to reduce overfitting, as demonstrated by the improvement over the results reported in rows two and four, for which training was performed from scratch. Figure 5 shows how the adaptation procedure with only an RL signal causes the student to diverge after some iterations. This is probably due to the increased length of the interaction (based on the curriculum strategy) that causes wrong gradient estimations. Table V shows the performance of ADATRAS in comparison with other trackers fine-tuned (following their original learning strategy) on $\mathcal{D}_{tr}^{(target)}$. Our approach results generally better. This can be attributed to the RL strategy, which leads to more efficient data exploration, ultimately providing a data augmentation effect.

Weak Supervision Analysis. Table VI reports the performances of ADATRAS adapted with different kind of supervision. The functions $\omega^{(iou)}(\cdot)$, $\omega^{(dist)}(\cdot)$ improve by a good margin the results achieved by learning from ground-truth bounding-boxes (GT $b_t^{(g)}$), or by learning just from the

TABLE VI: Performance of the proposed tracker under different supervision settings. Best results, per supervision method, are highlighted in bold.

Supervision	VisDrone		PTB-TIR		AquaBox	
	SS	PS	SS	PS	SS	PS
GT $b_t^{(g)}$	0.490	0.757	0.640	0.803	0.517	0.629
KD $b_t^{(t)}$	0.497	0.769	0.601	0.788	0.514	0.634
$\omega^{(iou)}(\cdot)$	0.552	0.823	0.661	0.862	0.576	0.732
$\omega^{(dist)}(\cdot)$	0.523	0.852	0.638	0.894	0.575	0.774

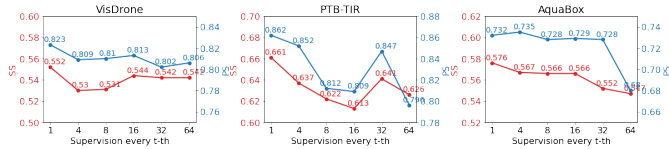


Fig. 6: Performance of ADATRAS trained on the three domains considering weak supervision delayed at different steps in time.

bounding-box predictions given by the teachers (KD $b_t^{(t)}$). Using $\omega^{(iou)}(\cdot)$ allows to achieve the best results in SS, while using $\omega^{(dist)}(\cdot)$ improves the PS performance. These results confirm that optimizing a specific performance measure as reward function induces the improvement of such measure at test time. Moreover, we analyzed the sensibility of ADATRAS to the weak supervision delayed in time. In particular, ADATRAS was trained with weak supervision happening every 4-th, 8-th, 16-th, 32-th, 64-th, temporal step t (in a 20 FPS setting, this would mean every 0.2, 0.4, 0.8, 1.6, 3.2, seconds). Results are shown in Figure 6. In general, performance tends to decrease as the supervision is more delayed, but without a significant loss, especially for domains with a larger number of frames (e.g. VisDrone). Interestingly, particularly delayed supervision allows achieving similar performance as the case in which supervision is given more frequently. We hypothesize this is due to the distribution between supervised $\mathcal{D}_{tr}^{(target)}$'s frames and the frames appearing in $\mathcal{D}_{te}^{(target)}$. More importantly, our proposed adaptation strategy reaches and surpasses the GT $b_t^{(g)}$ adaptation (row one of Table IV) even with delayed supervision.

Impact of Source and Teachers. Table VII reports the performance of ADATRAS which $s(\cdot|\theta)$ is adapted after learning on two different source domains. The performance of the two settings before adaptation are reported in the first two rows. $s(\cdot|\theta)$ trained on the GOT-10k dataset performs much better than $s(\cdot|\theta)$ optimized on the LaSOT dataset, due to the broader knowledge acquired on the larger GOT-10k. The results in rows three and four show that such a trend is maintained also after adaptation, showing that a better baseline tracking behavior is an important factor to achieve a better adapted tracking policy.

In Table VIII ADATRAS was analyzed after adaptation with different teacher setups. Using a better teacher does not translate into better performance, suggesting that it is important to understand on which sequences teachers perform well. Best results are obtained by learning from multiple teachers, demonstrating that the knowledge of these is compensated on $\mathcal{D}_{tr}^{(target)}$. Moreover, giving a ranking of teachers and selecting

TABLE VII: Performance comparison of ADATRAS adapted starting from different source domain knowledge. Performance without adaptation is also reported in the first two rows. Best results are highlighted in bold.

Source	VisDrone		PTB-TIR		AquaBox	
	SS	PS	SS	PS	SS	PS
no-adaptation - LaSOT	0.233	0.475	0.359	0.591	0.328	0.335
no-adaptation - GOT-10k	0.384	0.653	0.432	0.603	0.522	0.619
adaptation - LaSOT	0.475	0.726	0.646	0.860	0.541	0.719
adaptation - GOT-10k	0.552	0.823	0.661	0.862	0.576	0.732

TABLE VIII: Performance of the proposed tracker with different teacher setups. Best results, per setup, are highlighted in bold.

Teachers	VisDrone		PTB-TIR		AquaBox	
	SS	PS	SS	PS	SS	PS
\mathbf{T}_M	0.525	0.786	0.542	0.733	0.521	0.556
\mathbf{T}_S	0.467	0.731	0.576	0.774	0.582	0.642
\mathbf{T}_R	0.466	0.734	0.604	0.755	0.537	0.729
\mathbf{T}_P random selection	0.533	0.791	0.654	0.825	0.603	0.735
\mathbf{T}_P with Eq. (8)	0.552	0.823	0.661	0.862	0.576	0.732

the best for each training video, allows better performance on domains where teachers are better and more training frames are available (e.g. VisDrone and PTB-TIR). For some domain, selecting them randomly leads to almost equal performances than the ranking-based selection, probably due to the data distributions of $\mathcal{D}_{tr}^{(target)}$ and $\mathcal{D}_{te}^{(target)}$ which don't reflect the average performance of the teachers.

VI. CONCLUSIONS

In this paper, we present the first methodology for domain adaption of DRTs, which are fast but inaccurate methods. We achieve such a goal by proposing a weakly-supervised approach, thus reducing labeling effort. RL is used to express weak supervision as a scalar application-dependent and temporally-delayed feedback. KD is employed to achieve convergence, and to transfer knowledge from other trackers. Extensive experiments on five different domains and three machine setups demonstrate the effective usage for various robotic perception domains. Real-time speed is achieved on small embedded devices and on machines without GPUs. Accuracy is comparable to more powerful but slow state-of-the-art trackers.

REFERENCES

- [1] N. Papanikolopoulos, P. K. Khosla, and T. Kanada, "Vision and control techniques for robotic visual tracking," in *Proceedings. 1991 IEEE International Conference on Robotics and Automation*, 1991, pp. 857–864 vol.1.
- [2] J. Portmann, S. Lynen, M. Chli, and R. Siegwart, "People detection and tracking from aerial thermal views," in *Proceedings - IEEE International Conference on Robotics and Automation*. Institute of Electrical and Electronics Engineers Inc., sep 2014, pp. 1794–1800.
- [3] A. Geiger, P. Lenz, C. Stiller, and R. Urtasun, "Vision meets robotics: The KITTI dataset," *The International Journal of Robotics Research*, vol. 32, no. 11, pp. 1231–1237, sep 2013. [Online]. Available: <http://journals.sagepub.com/doi/10.1177/0278364913491297>
- [4] F. Shkurti, W. D. Chang, P. Henderson, M. J. Islam, J. C. G. Higuera, J. Li, T. Manderson, A. Xu, G. Dudek, and J. Sattar, "Underwater multi-robot convoying using visual tracking by detection," in *IEEE International Conference on Intelligent Robots and Systems*, vol. 2017-Sept. Institute of Electrical and Electronics Engineers Inc., dec 2017, pp. 4189–4196.
- [5] J. Luiten, T. Fischer, and B. Leibe, "Track to reconstruct and reconstruct to track," *IEEE Robotics and Automation Letters*, vol. 5, no. 2, pp. 1803–1810, apr 2020.

- [6] M. Dunnhofer, M. Antico, F. Sasazawa, Y. Takeda, S. Camps, N. Martinel, C. Micheloni, G. Carneiro, and D. Fontanarosa, "Siam-U-Net: encoder-decoder siamese network for knee cartilage tracking in ultrasound images," *Medical Image Analysis*, vol. 60, p. 101631, feb 2020.
- [7] D. Gordon, A. Farhadi, and D. Fox, "Re 3 : Real-time recurrent regression networks for visual tracking of generic objects," *IEEE Robotics and Automation Letters*, vol. 3, no. 2, pp. 788–795, 2018.
- [8] D. Held, S. Thrun, and S. Savarese, "Learning to Track at 100 FPS with Deep Regression Networks," *European Conference on Computer Vision*, vol. abs/1604.0, 2016. [Online]. Available: <http://arxiv.org/abs/1604.01802>
- [9] M. Dunnhofer, N. Martinel, and C. Micheloni, "Tracking-by-Trackers with a Distilled and Reinforced Model," in *Asian Conference on Computer Vision*, 2020.
- [10] J. Deng, W. Dong, R. Socher, L.-J. Li, Kai Li, and Li Fei-Fei, "ImageNet: A large-scale hierarchical image database," in *IEEE Conference on Computer Vision and Pattern Recognition*. IEEE, jun 2009, pp. 248–255. [Online]. Available: <http://ieeexplore.ieee.org/document/5206848/>
- [11] K. Chaudhary, M. Zhao, F. Shi, X. Chen, K. Okada, and M. Inaba, "Robust real-time visual tracking using dual-frame deep comparison network integrated with correlation filters," in *IEEE International Conference on Intelligent Robots and Systems*, vol. 2017-Septe. Institute of Electrical and Electronics Engineers Inc., dec 2017, pp. 6837–6842.
- [12] S. Reddy, M. Mathew, L. Gomez, M. Rusinol, D. Karatzas, and C. V. Jawahar, "RoadText-1K: Text Detection Recognition Dataset for Driving Videos," in *Proceedings - IEEE International Conference on Robotics and Automation*. Institute of Electrical and Electronics Engineers Inc., may 2020, pp. 11074–11080.
- [13] K. De Langis and J. Sattar, "Realtime Multi-Diver Tracking and Re-identification for Underwater Human-Robot Collaboration," in *Proceedings - IEEE International Conference on Robotics and Automation*. Institute of Electrical and Electronics Engineers Inc., may 2020, pp. 11140–11146.
- [14] A. Roy, X. Zhang, N. Wolleb, C. P. Quintero, and M. Jagersand, "Tracking benchmark and evaluation for manipulation tasks," in *Proceedings - IEEE International Conference on Robotics and Automation*, vol. 2015-June, no. June. Institute of Electrical and Electronics Engineers Inc., jun 2015, pp. 2448–2453.
- [15] B. Li, W. Wu, Q. Wang, F. Zhang, J. Xing, and J. Yan, "SIAMRPN++: Evolution of siamese visual tracking with very deep networks," *IEEE Conference on Computer Vision and Pattern Recognition*, vol. 2019-June, pp. 4277–4286, 2019. [Online]. Available: <http://arxiv.org/abs/1812.11703>
- [16] H. Nam and B. Han, "Learning Multi-domain Convolutional Neural Networks for Visual Tracking," *IEEE Conference on Computer Vision and Pattern Recognition*, vol. 2016-December, pp. 4293–4302, 2016.
- [17] M. Danelljan, G. Bhat, F. S. Khan, and M. Felsberg, "ATOM: Accurate Tracking by Overlap Maximization," in *IEEE Conference on Computer Vision and Pattern Recognition*, 2019. [Online]. Available: <https://github.com/visionml/pytracking.http://arxiv.org/abs/1811.07628>
- [18] G. Bhat, M. Danelljan, L. Van Gool, and R. Timofte, "Learning Discriminative Model Prediction for Tracking," in *Proceedings of the IEEE/CVF International Conference on Computer Vision*, 2019. [Online]. Available: <https://github.com/visionml/pytracking.http://arxiv.org/abs/1904.07220>
- [19] S. J. Pan and Q. Yang, "A survey on transfer learning," pp. 1345–1359, 2010.
- [20] G. Csurka, "A comprehensive survey on domain adaptation for visual applications," in *Advances in Computer Vision and Pattern Recognition*. Springer London, 2017, no. 9783319583464, pp. 1–35.
- [21] G. Angeletti, B. Caputo, and T. Tommasi, "Adaptive Deep Learning Through Visual Domain Localization," in *Proceedings - IEEE International Conference on Robotics and Automation*. Institute of Electrical and Electronics Engineers Inc., sep 2018, pp. 7135–7142.
- [22] J. Zhang, L. Tai, P. Yun, Y. Xiong, M. Liu, J. Boedecker, and W. Burgard, "VR-Goggles for Robots: Real-to-Sim Domain Adaptation for Visual Control," *IEEE Robotics and Automation Letters*, vol. 4, no. 2, pp. 1148–1155, apr 2019.
- [23] A. Carlson, K. A. Skinner, R. Vasudevan, and M. Johnson-Roberson, "Sensor Transfer: Learning Optimal Sensor Effect Image Augmentation for Sim-to-Real Domain Adaptation," *IEEE Robotics and Automation Letters*, vol. 4, no. 3, pp. 2431–2438, jul 2019.
- [24] M. Wulfmeier, A. Bewley, and I. Posner, "Addressing appearance change in outdoor robotics with adversarial domain adaptation," in *IEEE International Conference on Intelligent Robots and Systems*, vol. 2017-Septe. Institute of Electrical and Electronics Engineers Inc., dec 2017, pp. 1551–1558.
- [25] M. Mancini, H. Karaoguz, E. Ricci, P. Jensfelt, and B. Caputo, "Kitting in the Wild through Online Domain Adaptation," in *IEEE International Conference on Intelligent Robots and Systems*. Institute of Electrical and Electronics Engineers Inc., dec 2018, pp. 1103–1109.
- [26] K. Fang, Y. Bai, S. Hinterstoisser, S. Savarese, and M. Kalakrishnan, "Multi-task domain adaptation for deep learning of instance grasping from simulation," in *Proceedings - IEEE International Conference on Robotics and Automation*. Institute of Electrical and Electronics Engineers Inc., sep 2018, pp. 3516–3523.
- [27] M. R. Loghmani, L. Robbiano, M. Planamente, K. Park, B. Caputo, and M. Vincze, "Unsupervised Domain Adaptation through Inter-Modal Rotation for RGB-D Object Recognition," *IEEE Robotics and Automation Letters*, vol. 5, no. 4, pp. 6631–6638, oct 2020.
- [28] E. Bellocchio, G. Costante, S. Cascianelli, M. L. Fravolini, and P. Valigi, "Combining Domain Adaptation and Spatial Consistency for Unseen Fruits Counting: A Quasi-Unsupervised Approach," *IEEE Robotics and Automation Letters*, vol. 5, no. 2, pp. 1079–1086, apr 2020.
- [29] G. Hinton, O. Vinyals, and J. Dean, "Distilling the Knowledge in a Neural Network," in *Deep Learning Workshop NIPS 2014*, mar 2014. [Online]. Available: <http://arxiv.org/abs/1503.02531>
- [30] R. S. Sutton and A. G. Barto, *Reinforcement Learning: An Introduction*, 2nd ed. Cambridge, MA, USA: MIT Press, 2018.
- [31] R. S. Sutton, D. McAllester, S. Singh, and Y. Mansour, "Policy gradient methods for reinforcement learning with function approximation," in *Advances in Neural Information Processing Systems*, 2000, pp. 1057–1063. [Online]. Available: <https://dl.acm.org/citation.cfm?id=3009806>
- [32] A. Nair, P. Srinivasan, S. Blackwell, C. Alceick, R. Fearon, A. De Maria, V. Panneershelvam, M. Suleyman, C. Beattie, S. Petersen, S. Legg, V. Mnih, K. Kavukcuoglu, and D. Silver, "Massively Parallel Methods for Deep Reinforcement Learning," jul 2015. [Online]. Available: <http://arxiv.org/abs/1507.04296>
- [33] Y. Wu, J. Lim, and M. H. Yang, "Object tracking benchmark," *IEEE Transactions on Pattern Analysis and Machine Intelligence*, vol. 37, no. 9, pp. 1834–1848, sep 2015.
- [34] M. Dunnhofer, N. Martinel, G. L. Foresti, and C. Micheloni, "Visual Tracking by means of Deep Reinforcement Learning and an Expert Demonstrator," in *Proceedings of The IEEE/CVF International Conference on Computer Vision Workshops*, 2019. [Online]. Available: <http://arxiv.org/abs/1909.08487>
- [35] K. He, X. Zhang, S. Ren, and J. Sun, "Deep residual learning for image recognition," in *IEEE Conference on Computer Vision and Pattern Recognition*, vol. 2016-December, 2016, pp. 770–778.
- [36] S. Hochreiter and J. Schmidhuber, "Long Short-Term Memory," *Neural Computation*, vol. 9, no. 8, pp. 1735–1780, nov 1997. [Online]. Available: <http://dx.doi.org/10.1162/neco.1997.9.8.1735>
- [37] L. Huang, X. Zhao, and K. Huang, "GOT-10k: A Large High-Diversity Benchmark for Generic Object Tracking in the Wild," *IEEE Transactions on Pattern Analysis and Machine Intelligence*, pp. 1–1, oct 2019. [Online]. Available: <http://arxiv.org/abs/1810.11981>
- [38] H. Fan, L. Lin, F. Yang, P. Chu, G. Deng, S. Yu, H. Bai, Y. Xu, C. Liao, and H. Ling, "LaSOT: A High-quality Benchmark for Large-scale Single Object Tracking," in *IEEE Conference on Computer Vision and Pattern Recognition*, sep 2019. [Online]. Available: <http://arxiv.org/abs/1809.07845>
- [39] D. Du *et al.*, "VisDrone-SOT2019: The vision meets drone single object tracking challenge results," in *Proceedings - 2019 International Conference on Computer Vision Workshop, ICCVW 2019*, 2019, pp. 199–212. [Online]. Available: <http://www.aiskyeye.com/>.
- [40] Q. Liu, Z. He, X. Li, and Y. Zheng, "PTB-TIR: A Thermal Infrared Pedestrian Tracking Benchmark," *IEEE Transactions on Multimedia*, vol. 22, no. 3, pp. 666–675, mar 2020.
- [41] D. P. Kingma and J. Ba, "Adam: A Method for Stochastic Optimization," *CoRR*, vol. abs/1412.6, 2014. [Online]. Available: <http://arxiv.org/abs/1412.6980>
- [42] M. Kristan *et al.*, "The Seventh Visual Object Tracking VOT2019 Challenge Results," in *Proceedings of the IEEE/CVF International Conference on Computer Vision Workshops*, 2019.
- [43] M. Kristan, A. Leonardis, J. Matas, M. Felsberg, R. Pflugfelder *et al.*, "The eighth visual object tracking vot2020 challenge results," in *Computer Vision – ECCV 2020 Workshops*, A. Bartoli and A. Fusiello, Eds. Cham: Springer International Publishing, 2020, pp. 547–601.